Phase-Separation Process and Self-Organization of Textures in the Biphase Region of Thermotropic Liquid Crystalline Poly(4,4′-dioxy-2,2′-dimethylazoxybenzene–dodecanedioyl). 1. A Study on the Athermal Conditions

Akemi Nakai,† Wei Wang, and Takeji Hashimoto*

Division of Polymer Chemistry, Graduate School of Engineering, Kyoto University, Kyoto 606–01, Japan

Alexandre Blumstein

Polymer Science Program, Department of Chemistry, University of Massachusetts Lowell, Lowell, Massachusetts 01854

Yoji Maeda

National Institute of Materials and Chemical Research, 1–1 Higashi, Tsukuba, Ibaraki 305, Japan

Received April 29, 1994; Revised Manuscript Received August 18, 1994®

ABSTRACT: The phase-separation process and the self-organization of the textures in the biphase region of a thermotropic liquid crystalline polyester sample [poly(4,4′-dioxy-2,2′-dimethylazoxybenzene–dodecanedioyl)] were studied by polarizing light microscopy both during the heating from the fully anisotropic phase to the biphase region and during the cooling from the isotropic phase to the biphase region. The phase separation occurs as a consequence of chain segregation according to the chain length. The phase-separation process is found to be the same for both thermal procedures, but the self-organization of the textures is found to strongly depend on thermal history. The domain structure depends on the thermal history under the heating and cooling cycles employed in this work. The special heating process used in this work developed a fractionation of molecular species in space according to their molecular length which caused a memory effect in the structure evolution during a subsequent cooling process, giving rise to a unique domain structure as described in the text.

I. Introduction

The poly(4,4′-dioxy-2,2′-dimethylazoxybenzene–dodecanedioyl) {IUPAC name: poly[oxy(3-methyl-1,4-phenylene)azoxy(2-methyl-1,4-phenylene)oxy(1,12-dioxo-1,12-dodecanediyl)]} is a thermotropic liquid crystalline (LC) polyester with a nematic nature which was first synthesized by A. Blumstein, R. B. Blumstein, and co-workers.[1–3] The chemical structure of the repeating unit of this polymer is shown below. It has a melting temperature of 121 °C

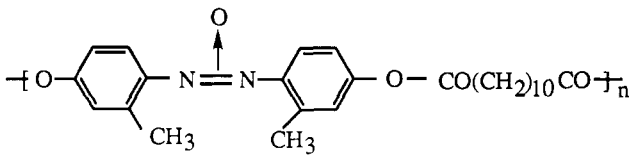

and a clearing temperature of 164 °C when $\overline{M}_n = 1.8 \times 10^4$. These temperatures depend on the degree of polymerization DP.[3] The liquid crystalline properties and the phase behavior of DDA-9 and related polymers are reviewed by one of the present authors.[4]

For the main-chain LC polymers an important property is that a biphase region wherein the isotropic and anisotropic phases coexist appears below the clearing temperature for thermotropic ones[5–16] or beyond the critical concentration for lyotropic ones.[17–19] The theoretical[20–24] and experimental[5–16] investigations indicate that the variations of the transition temperature and of the breadth of the transition interval are strongly related to the size distribution of rigid macromolecules and the distribution of mesogens on the main chain. For low DP's the nature of the end groups is also an important factor. For some LC copolyesters a wide biphase region was observed which was mainly considered as a consequence of heterogeneity in composition of the main chain.[11–13] For DDA-9 and some related LC polyesters, a relatively narrow biphase region was found.[7–10,15] Polarizing light microscopy, differential scanning calorimetry (DSC), nuclear magnetic resonance (NMR), and others were used to determine the chain segregation or demixing between the isotropic and anisotropic domains in the biphase region.[4] In these studies the formation of the biphase region was confirmed, for example, from isotropization or anisotropization temperatures. The biphase formation was proposed to be attributable to selective partitioning of chain lengths between the anisotropic and isotropic domains.[4,7–10,16] However, phase-separation processes and mechanisms and dynamical evolution of the domain structures in the biphase region are far from being understood. Thus in this work we aimed to conduct detailed morphological studies concerning the self-organization of textures in the biphase region by using polarizing light microscopy.

As suggested in the previous work,[4,7–10] we refer to the chain segregation and phase-separation processes as a process of formation and growth of the isotropic phase in the matrix of the anisotropic phase, when the temperature is raised from a fully anisotropic phase to the biphase region. In the biphase region, a part of the molecular

† Present address: Department of Home Economics, Kyushu Women's Junior College, 1–1 Jiyugaoka, Yawatanishi, Kitakyushu 807, Japan.

® Abstract published in *Advance ACS Abstracts,* October 1, 1994.

0024-9297/94/2227-6963$04.50/0

species of the LC polyester having a shorter chain length than the other cannot be incorporated into the nematic phase and hence is segregated out from the nematic phase to form small domains in which the molecules are expected to be essentially in random-coiled conformations. The domains' growth or the self-organization of textures is a consequence of the diffusion–coalescence process driven by interfacial tension between the isotropic domains and the anisotropic domains. This process leading to a biphase equilibrium is regarded to be a phase-separation process. We expect that the phase-separation process may induce the domain formation or fractionation of the molecular species in space according to molecular weights, i.e., the anisotropic domains having a higher average molecular weight than the isotropic domains.[4,7-10,16] We show that the chain segregation and phase-separation processes and the self-organization of textures also occur upon cooling of the LC polyester from the isotropic to the biphase region.

One of the advantages of using DDA-9 as a sample is that the LC polyester has relatively low melting and clearing temperatures; thus, all the experiments can be done in the low temperature interval in which the chemical decomposition can be mostly avoided. Another is that DDA-9 has an orderly sequence of rigid and flexible units in the main chain. The transesterification cannot change this sequence, if it occurs during the experiment. We will divide our results into two parts. In this paper we will present the results concerning the chain segregation and phase-separation processes and the self-organization of textures under athermal conditions. In the following paper we will discuss these processes during isothermal annealing and the liquid crystalline texture of this polyester in the biphase region.[25]

II. Experimental Section

Poly(4,4′-dioxy-2,2′-dimethylazoxybenzene–dodecanedioyl) was prepared according to the method described elsewhere.[1-3] It has a number-average molecular weight $\overline{M}_n = 2 \times 10^4$ and a heterogeneity index $\overline{M}_w/\overline{M}_n = 2.7$. The heterogeneity index was determined by gel permeation chromatography (Waters GPC 150 C with a RI detector) in chloroform at 40 °C. This LC polyester in the solid state has a yellow color. The sample was dried in vacuum for a day at room temperature in order to remove the moisture. Film samples for optical microscopy were prepared by pressing a small sample of the polymer between two clear glass slides on a heating stage. The typical thickness of the sample is 20 μm. The sample was pressed at a temperature of 167 °C which is approximately 5 °C higher than its clearing temperature and then annealed at this temperature for 1 h in order to eliminate the effect of sample history. The phase-separation process in the biphase region was observed by a polarizing light microscope (PLM) (Nikon Optiphot-Pol) with crossed polarizers between which a red plate with retardation in 530 nm was inserted and with a heating–cooling stage (Linkam Th-600). In order to determine the fraction of the isotropic phase and the size of the anisotropic droplets, micrographs were first digitized by using a scan program (Apple Scan), and then the digitized data were analyzed by using image analysis programs (NIH Image 1.53 and Adobe Photoshop 2.5).

Three quite different thermal programs which are schematically shown in Figure 1 were used in this study in order to detect the chain segregation and phase-separation processes and the self-organization of textures. The parameters characterizing the thermal programs are summarized in Table 1. These parameters were chosen in order to avoid the effect of transesterification of DDA-9.[26] In Figure 1, part a demonstrates an experimental procedure for detecting the formation of the biphase region through phase separation from the fully liquid crystalline phase during the heating process, part b that for detecting the formation of the biphase region through phase separation from the isotropic

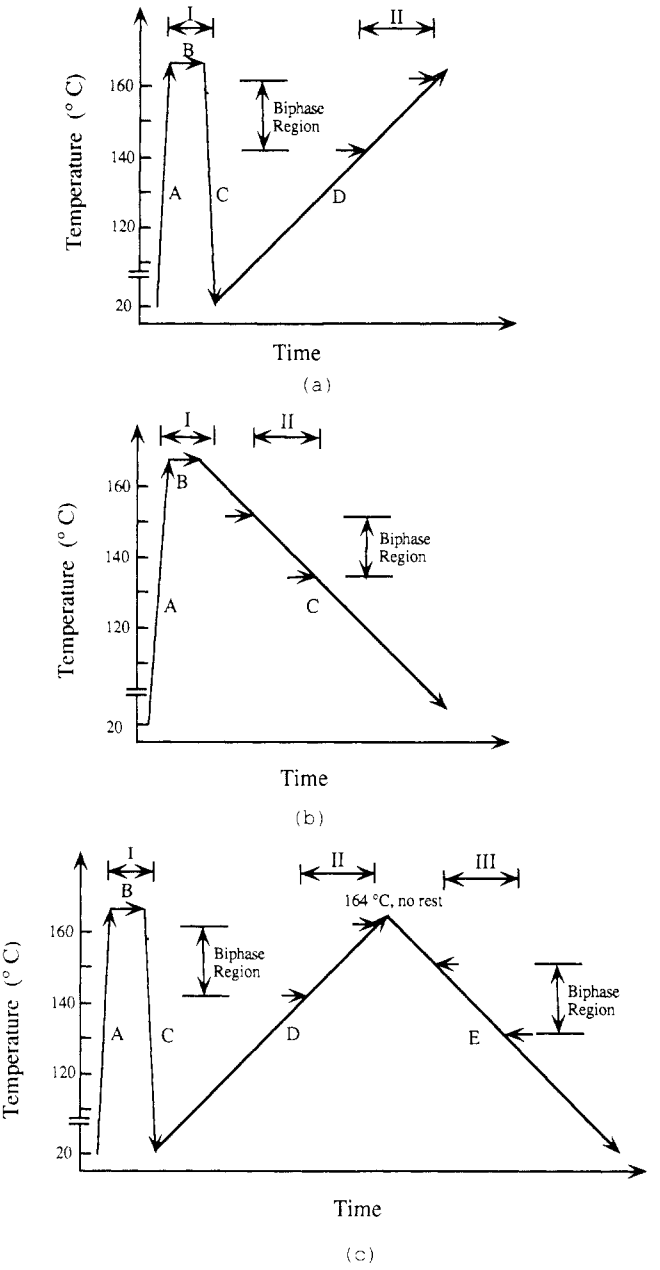

Figure 1. Two temperature programs (a and b) used in this study for investigating the chain segregation and phase-separation processes during the heating process (a) and the cooling process (b) of a film sample, and the program (c) involving both the heating and cooling processes which is aimed to explore a memory effect. All the parameters characterizing the thermal programs are summarized in Table 1.

Table 1. Parameters Characterizing the Thermal Programs Shown in Figure 1

	program in part a	program in part b	program in part c
A	>100 °C/min	>100 °C/min	>100 °C/min
B	167 °C for 1 h	167 °C for 1 h	167 °C for 1 h
C	>100 °C/min	1 °C/min	>100 °C/min
D	1 °C/min		1 °C/min
E			1 °C/min

phase during the cooling process, and part c that for investigating the influence of the memory effect on the phase separation; this influence can be studied by comparing the phase separations in region III in part c with those in region II in part b. Region I in Figure 1 reflects the sample preparation. In region II the phase-separation process for a fresh sample was detected. Effects of thermal history on phase separation can be studied by comparing the phase-separation process during heating and cooling processes for the same sample.

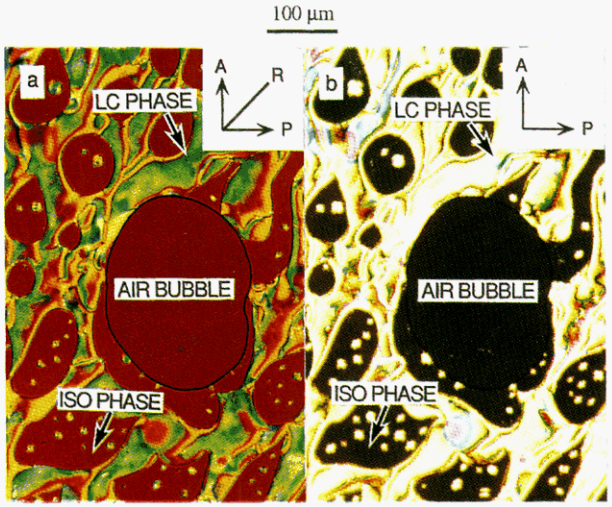

Figure 2. Micrographs of a DDA-9 sample in the biphase region (at 148 °C) showing the anisotropic phase (LC PHASE), the isotropic phase (ISO PHASE), and an air bubble; (a) with crossed polarizers (designated as P and A) and red plate (designated as R); (b) with crossed polarizers only.

III. Results

A. Distinction between Isotropic Areas and Air Bubbles. The phase-separation process of the LC polyester within the biphase region can be easily detected by polarizing light microscopy (PLM), since isotropic and anisotropic melts have a strong contrast when viewed under crossed polarizers. It is, however, difficult to distinguish the isotropic melt and air bubbles that could occasionally appear in the sample, since they are optically isotropic and appear dark. The difficulty can be overcome by inserting a red plate (with retardation in 530 nm) between the crossed polarizers. Figure 2 shows two color micrographs which were taken by PLM with (Figure 2a) and without (Figure 2b) the red plate (designated as R hereafter in all the micrographs) for a DDA-9 film in the biphase region between two glass slides. These micrographs show a texture of the sample containing the liquid crystalline phase (designated as LC PHASE), the isotropic melt (designated as ISO PHASE), and an air bubble. The bright areas which usually are yellow or green are obviously the liquid crystalline phase. The isotropic areas are red in Figure 2a and black in Figure 2b. The air bubble appears dark in Figure 2b as the isotropic phase does, so that a clear distinction between them is not easy in this situation. However, when the temperature is lowered, the isotropic area is transformed into the anisotropic phase, causing either a color change or a brightness change (from dark to bright), as will be discussed in more detail later. This provides a way to distinguish indirectly between the two. In Figure 2a, however, the color of the isotropic melt is slightly different from that of the air bubbles. This provides a direct method to distinguish between the two. Another important feature of the air bubbles is that a dark loop can be easily observed on their edge area when the red plate is used. Another advantage to using the red plate is that the influence of the dark brushes due to the disclinations which often appear in nematic samples can be avoided. Owing to these reasons, we usually used the polarizing light microscope with crossed polarizers and a red plate in this study. It should be emphasized that the air bubble shown in Figure 2 was not induced by chemical decomposition of the polymer but was artificially formed during the preparation of the film sample by pressing.

B. Phase Separation during the Heating Process. In contrast to the vast majority of random LC copolyesters,[11-13] DDA-9 shows a relatively narrow biphase region. When compared to some rigid–flexible polyesters, however, the biphase region of DDA-9 does not have an exceedingly narrow biphase interval. In fact, it has a biphase interval significantly larger than AZA-9 (a polyester with azalaic acid spacer $n = 7$) and other odd-spacered polymers.[8] Some ordered polymers mentioned by Stupp and co-workers[11,12] have also a narrower biphase interval. A heating rate of 1 °C/min was used in this work to determine the temperature interval within which the biphase region occurs in the heating cycle. Under this condition the isotropic phase starts to develop in the matrix of the anisotropic phase at 143 °C as shown in Figure 3a; it grows with temperature (and of course with time), and the anisotropic phase totally disappears at 162 °C as shown in Figure 3h. Hereafter we designate the transition temperature from the anisotropic phase to the biphase region as $T_{NN\rightarrow NI}$ and the transition temperature from the biphase region to the isotropic phase as $T_{NI\rightarrow II}$. The temperature interval within which isotropic and anisotropic phases coexist is approximately 20 °C, much narrower when compared with that (120 °C) for random LC copolyesters.[11-13] It is, however, necessary to point out that the width of the biphase region studied is not the equilibrium biphase width as studied under conditions described in ref 8 but is that observed under the thermal history reported in this paper.

The separation process of the isotropic phase from the anisotropic phase upon increasing the temperature is shown by a series of micrographs in Figure 3. The fraction of the isotropic phase, x_I, and the number of isotropic domains per square millimeter, N_{ISD}, measured as a function of temperature, T, from the micrographs, some of which are shown in Figure 3, are shown in Figure 4. A crystalline texture of the DDA-9 sample prepared by quenching it from 167 °C to room temperature was observed, although not shown in Figure 3. This texture does not vary until the melting temperature, T_m, which is 118 °C. In the fully anisotropic melt region, the texture of the sample varies with the increase of the temperature primarily due to the annihilation of defects.[13,27-29] At the temperature slightly above $T_{NN\rightarrow NI}$, some isotropic droplets were observed in the matrix of the anisotropic phase, indicating that the isotropic phase starts to separate from the anisotropic phase, as shown Figure 3a. At first some small red droplets appear in the bright anisotropic phase. With increasing the temperature, more and more red droplets gradually appear and at the same time their size increases, as shown in Figure 3b. The temperature interval of DDA-9 for this stage is approximately 4 °C between 143 and 147 °C. This stage is designated as an initial stage of the isotropic phase separating from the anisotropic phase.

The next stage, represented by parts c and d of Figure 3, appears to show the following ordering processes. As temperature is further raised, more new isotropic droplets are formed in the anisotropic medium. Their size grows mainly as a result of diffusion–coalescence process driven by interfacial tension between the isotropic and anisotropic regions. These two processes, i.e., increased volume fraction of the isotropic phase and the coarsening of the isotropic droplets as quantitatively shown in Figure 4, converge to form the percolated network composed of the anisotropic phase in the matrix of the isotropic phase. The network formed grows with a dynamical self-similarity[30-32] as shown in parts d and e of Figure 3 toward formation of the network with a larger mesh size. This self-similar growth is primarily driven by interfacial tension

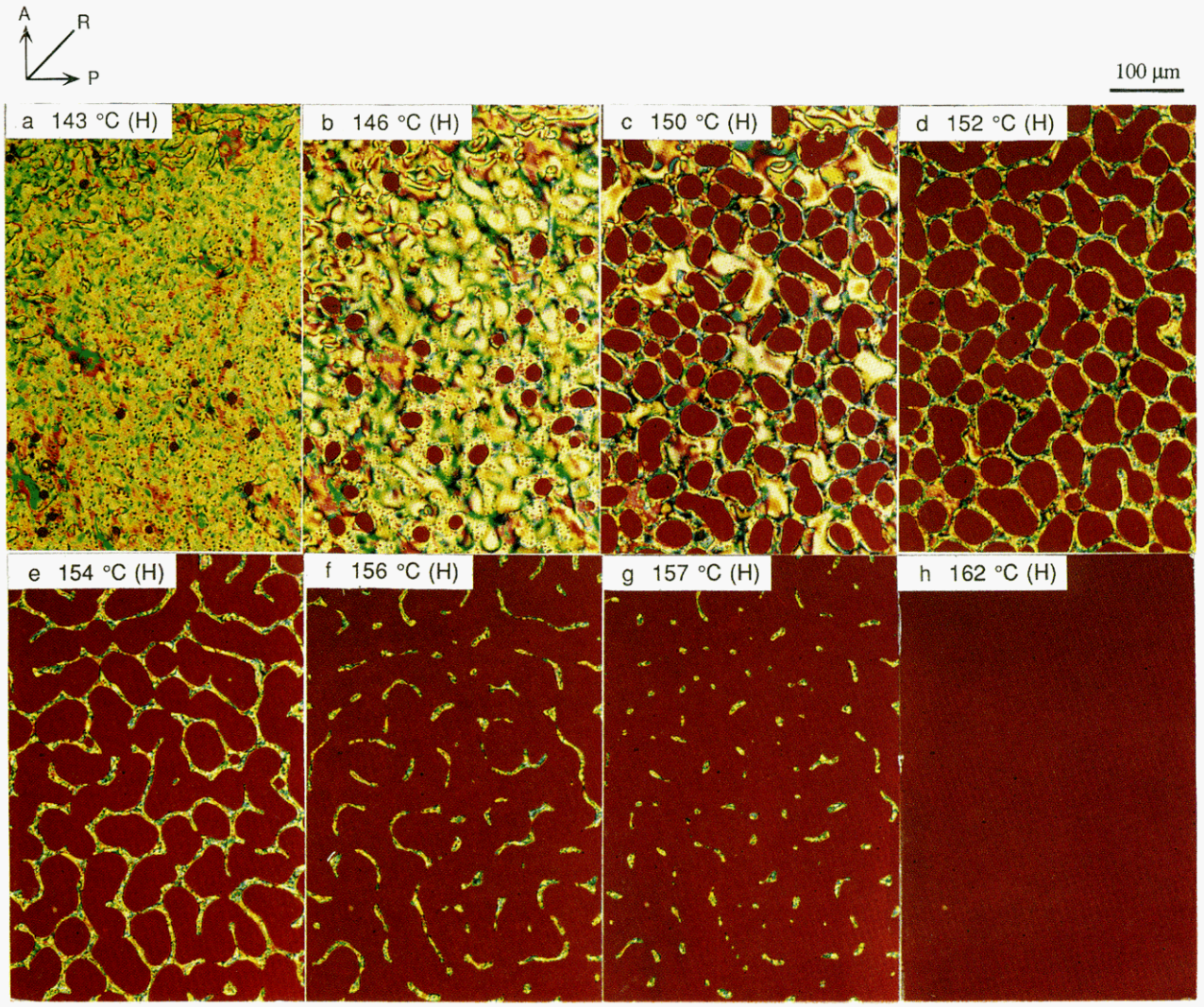

Figure 3. Micrographs showing the phase-separation process of a fresh DDA-9 sample heated from a fully anisotropic state during heating at a rate of 1 °C/min. A series of micrographs focus on the same area of the same sample.

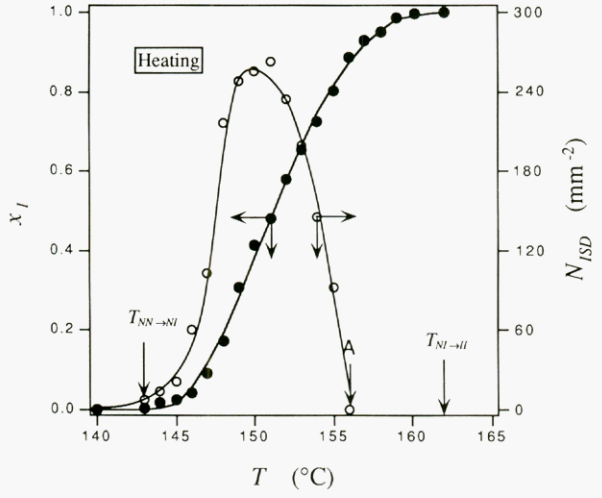

Figure 4. Fraction of the isotropic phase, x_I, and a number of isotropic domains, N_{ISD}, as a function of temperature. x_I and N_{ISD} were measured from the micrographs, some of which are shown in Figure 3.

and involves the breakup of portions of the network which happen to become thin due to thermal motion, and the broken-up portions of the network are absorbed in the rest of the network to make it thicker. In this way the mean curvature of the interface and interface area decrease. It should be noted that the growth of the network is counterbalanced by the decrease in the volume fraction of the anisotropic phase $(1 - x_I)$. The temperature interval for this stage is approximately 6 °C between 147 and 153 °C.

As the temperature is further raised, more and more molecular species are segregated from the anisotropic phase into the isotropic phase. As a consequence, the fraction of the isotropic phase increases with temperature, as clearly shown in the x_I–T relation in Figure 4. The anisotropic phase which continues to decrease below 50% cannot maintain a macroscopically percolated network. This induces the following dynamical evolution of texture: first formation of a locally percolated network, subsequently a network composed of fragmented long anisotropic threads as shown in Figure 3f, and eventually clusters of anisotropic droplets as shown in Figure 3g. N_{ISD} falls down to zero as pointed out by arrow A in Figure 4, since there the isotropic phase becomes a continuous medium. The dynamical percolation-to-cluster transition of the anisotropic network[27,32] can be characterized by the decrease of N_{ISD}. The long anisotropic threads become unstable and burst into a series of anisotropic droplets along the thread axes as shown in Figure 3g, analogous to Tomotika's instability.[33] A spatial distribution of the droplets is regular as it results from the regular network structure. This stage occurs in a temperature interval between 157 and 162 °C for DDA-9. Finally the liquid crystalline

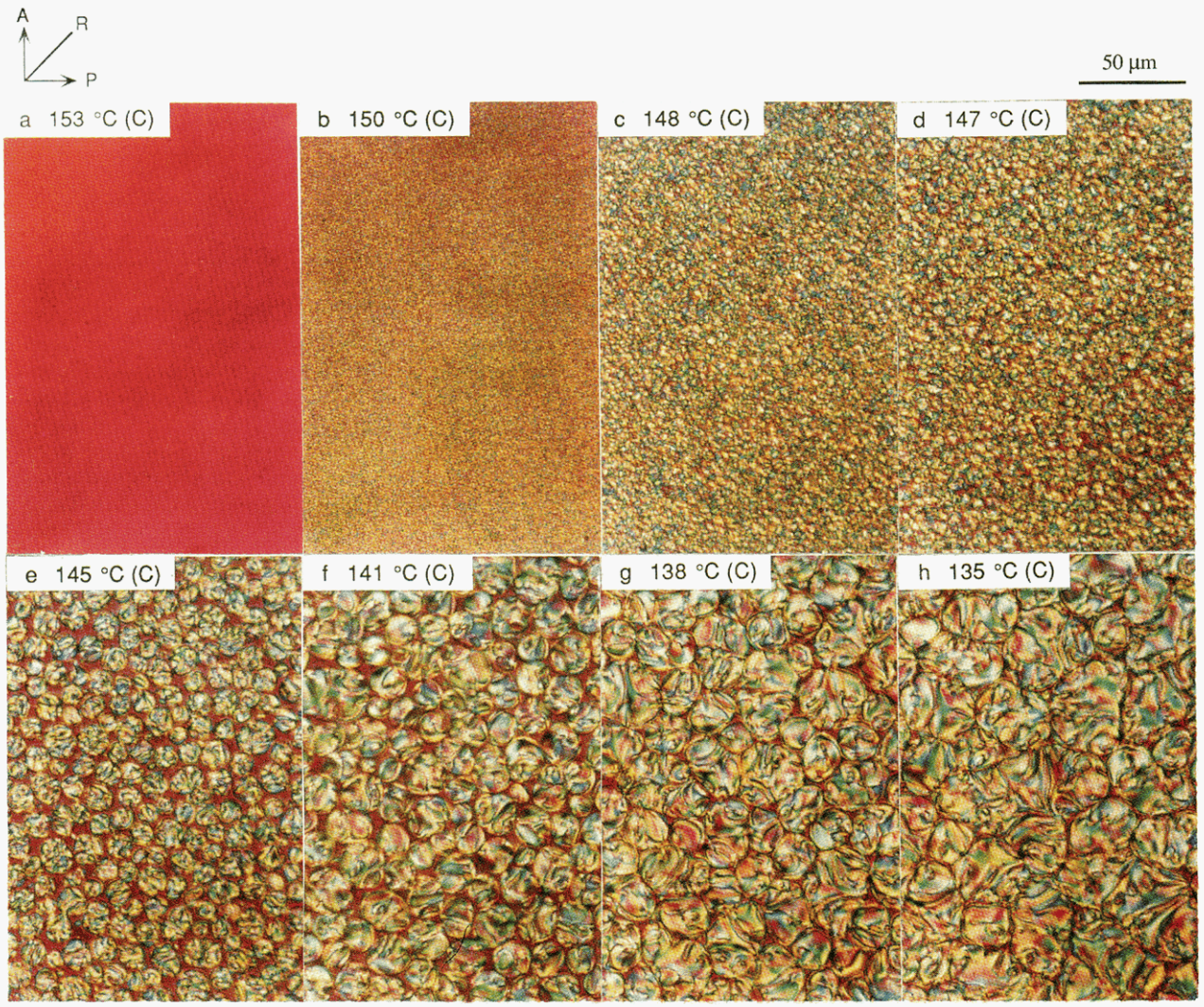

Figure 5. Micrographs showing the phase transition and the phase separation on cooling of a fresh sample from the isotropic phase at a rate of 1 °C/min. The micrographs are obtained from the same area of the same sample.

droplets disappear when temperature increases to 162 °C ($T_{NI\rightarrow II}$).

C. Phase Separation during the Cooling Process. As mentioned above the clearing temperature for DDA-9 is 162 °C which is relatively lower than that for some LC copolyesters.[11-13] This characteristic gives us a chance to study the phase-separation process and the self-organization of textures in the biphase region when the polymer sample is cooled down to this region from the isotropic state. This kind of study cannot be achieved for some LC copolyesters[11-13] having a high clearing temperature, which sometimes is higher than their decomposition temperature.

Owing to supercooling of the DDA-9 isotropic melt, the anisotropic phase starts to develop from the isotropic phase at 151 °C which is approximately 10 °C lower than $T_{NI\rightarrow II}$ (as schematically illustrated in Figure 1). Hereafter this temperature is designated as $T_{II\rightarrow IN}$. The development of the textures and the phase behavior of the DDA-9 film sample during cooling at a rate 1 °C/min observed by PLM with the red plate are shown by a set of micrographs in Figure 5. Correspondingly, the relationship between the fraction of the isotropic phase, x_I, and temperature and that between the diameter of the anisotropic droplets, D_{AN}, and temperature obtained from the micrographs, some of which are shown in Figure 5, are drawn in Figure 6. From Figure 5a we can see that the sample is in the isotropic state when it was cooled down to 153 °C. The first sign of formation of the anisotropic phase is that

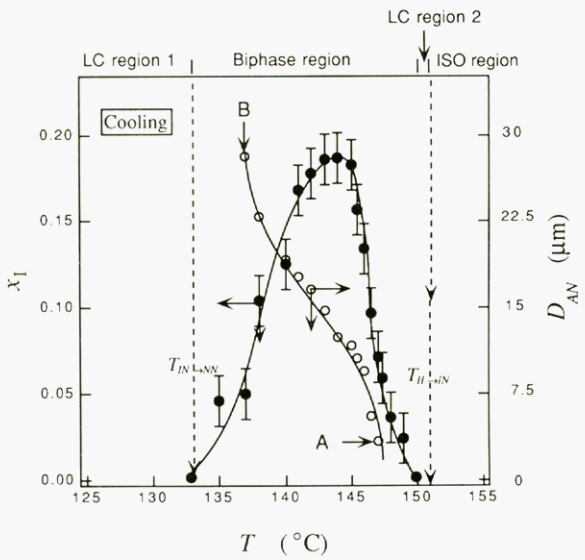

Figure 6. Fraction of isotropic phase, x_I, and the diameter of the anisotropic droplets, D_{AN}, as a function of temperature during cooling from the isotropic phase. x_I and D_{AN} were measured from the micrographs, some of which are shown in Figure 5.

many very small bright particles instantaneously and uniformly appear in the whole view as shown in Figure 5b. The particle size quickly increases and correspondingly

their number decreases. This indicates that the growth of a particle is due to a diffusion and coalescence of the adjacent particles. This change occurs within a narrow temperature range between 151 and 150 °C. Between 150 and 148 °C a seemingly fully anisotropic phase is observed by PLM, indicating that the isotropic phase is first transformed into the anisotropic phase. The process of phase transition at this stage is shown in parts b and c of Figure 5. The micrograph in Figure 5c shows a texture in which the fraction of the anisotropic phase is close to 1.

When the temperature is lowered from 148 °C, some isotropic domains that can be identified as red areas between the anisotropic droplets appear in the sample, as shown in Figure 5d. This indicates that chain segregation and concomitant phase separation start to occur at a level discernible by optical microscopy, leading to formation of a vast number of anisotropic droplets. This process is clearly characterized by the relation between x_I and temperature in the interval between 148 and 144 °C. In this temperature interval the fraction of the isotropic melt increases with a decrease of the temperature. This further indicates that the rate of separation of isotropic and anisotropic phases, R_{PS}, is faster than that of the isotropic phase being transformed into the anisotropic phase, R_{PT}, due to a decrease of temperature. When the temperature decreases further to 143 °C, a peak is found in the relation between x_I and temperature, indicating that at this temperature a balance between R_{PS} and R_{PT} is reached. Then x_I decreases with a decrease of temperature until entering the fully anisotropic region at a temperature of 133 °C (this temperature is designated hereafter as $T_{IN\rightarrow NN}$), demonstrating that R_{PS} is outweighed by R_{PT} and eventually decreases to zero at 133 °C. The latter transformation from the isotropic to anisotropic phase is accelerated by a decrease of the temperature.

The change in size, D_{AN}, of the anisotropic droplets with decreasing the temperature is also shown by unfilled circles in Figure 6. Owing to the isotropic phase separating from the fully anisotropic phase at 148 °C, an anisotropic droplet starts to form. This is indicated by an arrow A in Figure 6. The LC texture of the sample is shown in parts d–g of Figure 5. It is worth noting that the isotropic phase does not form droplets but becomes a continuous phase, despite the fact that its fraction is typically lower than 0.2. The size of the anisotropic droplets increases when the temperature is reduced from 147 to 137 °C, mainly due to the diffusion–coalescence process of droplets as a result of a decrease of the interfacial tension between the isotropic and anisotropic phases. The droplet size is strikingly uniform. After the formation of the anisotropic droplets, first their size increases rapidly with lowering of the temperature and then the growth rate ($|dD_{AN}/dT|$) slows down and reaches a minimum at the temperature at which the highest fraction of the isotropic phase is attained. This indicates that the isotropic melt separating from the anisotropic phase obstructs the diffusion–coalescence of anisotropic droplets to a certain extent. At temperatures lower than 143 °C the growth rate of anisotropic droplets increases again as the isotropic melt which has separated from the anisotropic phase is retransformed into an anisotropic phase, owing to a decrease of the temperature. At 137 °C a continuous anisotropic phase is formed, as pointed out by an arrow B in Figure 6.

The coalescence process between the anisotropic droplets is quite different from that between the isotropic droplets. The coalescence generally involves the two droplets coming into contact and then being welded into a larger droplet. The coalescence between two adjacent anisotropic droplets appears to occur only if the director orientation in the area of contact is matched. It is observed that some of the droplets in contact keep their individuality for a long time but some are rapidly welded into larger ones. Even after the coalescence, the memory of the droplet boundary is preserved for some time as defects in the anisotropic phase. This coalescence process will be discussed in more detail in the following paper.[25]

The results obtained in this and the last sections clearly indicate that the phase-separation process occurring during cooling of an isotropic melt to the biphase region is quite different from that occurring during heating of a fully anisotropic melt to the biphase region. One of the significant differences is that, when an isotropic melt is cooled down to the biphase region, the phase separation follows a phase transition from the isotropic phase to the anisotropic phase. This LC state (LC region 2 in Figure 6) formed from the isotropic state during the cooling process is an unstable LC state of which properties will be discussed later and should be distinguished from the fully anisotropic state at $T \leq T_{IN\rightarrow NN}$ (LC region 1 in Figure 6). We designate this LC region as a stable LC region.

D. Memory Effect. Micrographs in Figure 7 that were taken in the same area of the same sample according to the temperature program shown in part c of Figure 1 show an influence of the memory effect on the phase transition and the phase separation of the DDA-9 sample in the biphase region. Figure 8 shows the change of the domain structure upon further lowering the temperature. Parts a and b of Figure 7 show a development of the texture in the late stage of the phase separation during the heating process, and Figure 7c indicates that the sample is in the isotropic state at 164 °C (corresponding to Figure 3h). A small anisotropic foreign particle which is stationary and clearly seen at the upper left corner in Figure 7 (clearly identified in Figure 7c) provides a target for the relative position of dynamically evolving domain structure. When this sample was cooled down again from this temperature at a rate of 1 °C/min, we observed a totally different behavior of the phase transition and the phase separation from the behavior of Figure 5.

At first we observed that some anisotropic, very small particles appear at 155 °C and then they form anisotropic domains at 2 or 3 °C lower than 155 °C, as shown in Figure 7d. The position of the domains newly appearing in Figure 7d is essentially the same as that of the anisotropic droplets seen in Figure 7b. Although the anisotropic droplets in Figure 7b are transformed into isotropic droplets and disappear at 162 °C as shown in Figure 7c at 164 °C, a memory of the droplets is conserved through the cooling process, and the anisotropization starts to occur from these domains. When the temperature continuously decreases, the anisotropization progresses from the center of the domain toward its periphery, giving rise to larger anisotropic domains as seen in the change of the image from part d to part e of Figure 7. The growth of the anisotropic domain is schematically illustrated in Figure 9 by a change from domains D_1 to D_2. Inside the anisotropic domains D_1, very small anisotropic droplets appear as seen in parts d and e of Figure 7 and as schematized in Figure 9 by the anisotropic droplets R_{L1}, as a consequence of chain segregation and phase separation in the domains D_1. This process seems to be identical to that observed homogeneously in the whole sample space in Figure 5, e.g., in the images in parts c–f of Figure 5. As the temperature is lowered (or time elapses), the domains D_1 grow to larger ones D_2 and the droplets inside the domains R_{L1} coalesce

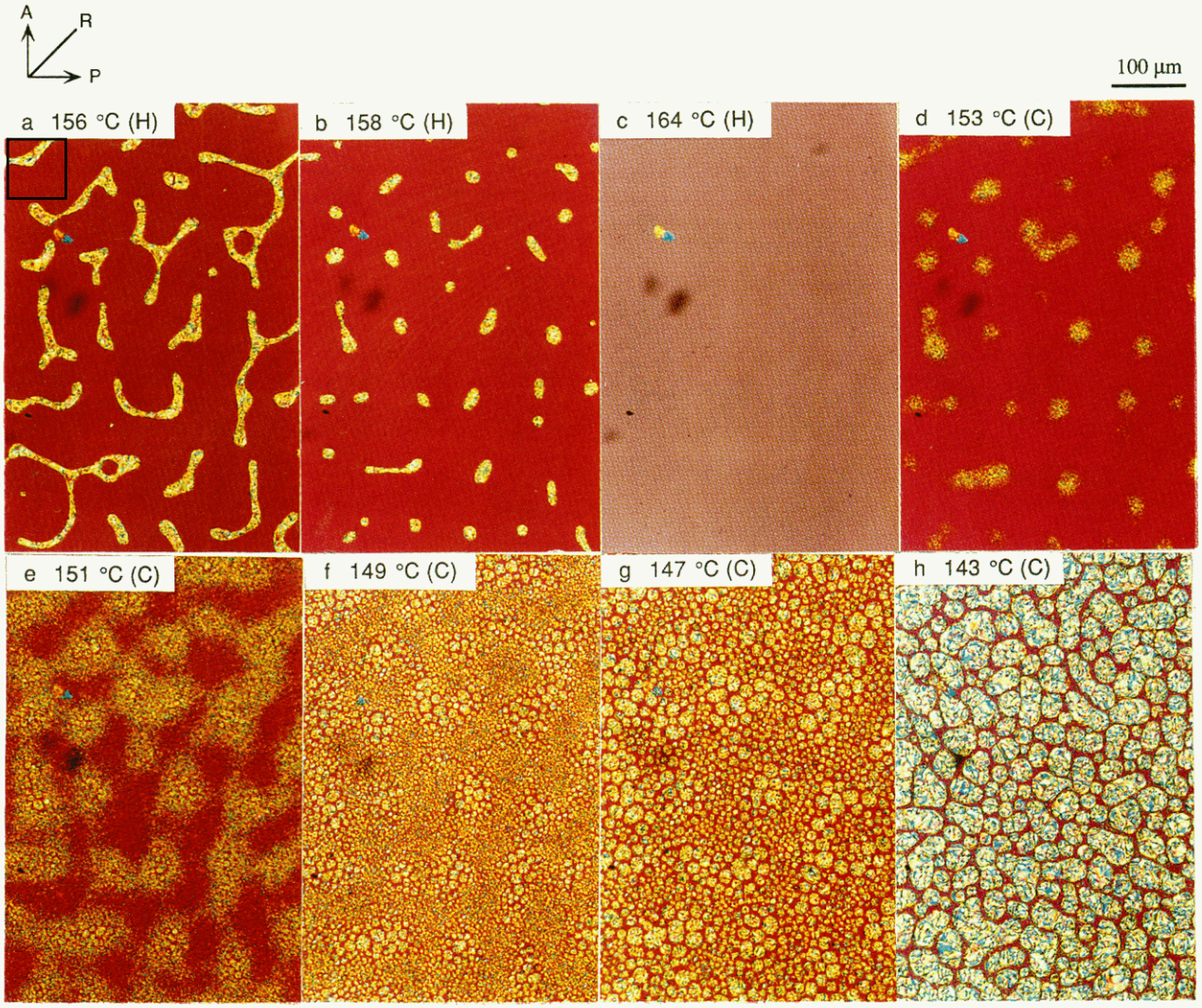

Figure 7. Micrographs showing the influence of the memory effect on phase transition and phase separation. The sample was treated according to the temperature program in part c of Figure 1. The micrographs are obtained from the same area of the same sample.

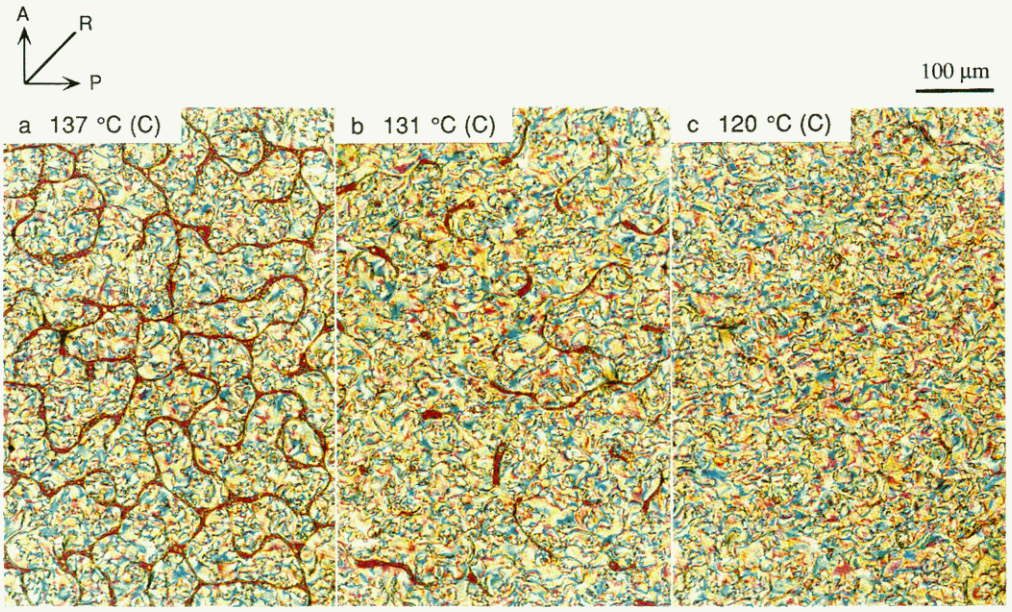

Figure 8. Micrographs showing a further change of domain structure on cooling for the sample shown in Figure 7. The micrographs were obtained on the same area as shown in Figure 7.

into larger droplets R_{L2} as schematized in Figure 9 and as seen in Figure 7e. The anisotropic droplets are surrounded by the isotropic phase A_i within the domains D_1 and D_2 (Figure 9). In Figure 7e we observe that the size of the droplets in the domains is polydisperse: the size of the droplets in the middle of the domains is larger than that

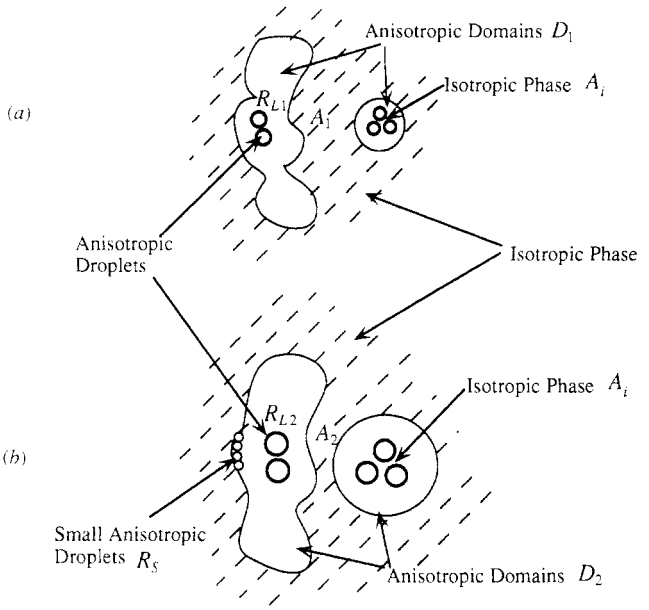

Figure 9. Schematic diagrams showing the growth of the anisotropic domains from D_1 to D_2 and the anisotropic droplets in the domains from R_{L1} to R_{L2}. These diagrams correspond to the growth shown in parts d and e of Figure 7.

of the droplets in the edge of the domains, as schematized in Figure 9b by the droplets R_{L2} and R_S. This is simply because the anisotropization in the edge of the domains occurred at a later time than that in the middle of the domains and the phase separation in the edge corresponded to an earlier stage than that in the middle. The shape of the domains in Figure 7e is close to the shape of the anisotropic droplets shown in Figure 7a.

The processes of the anisotropization upon lowering the temperature make the isotropic region between the anisotropic domains become narrower, as schematized by the change of the region from A_1 to A_2 in Figure 9. Eventually the whole sample space is full of anisotropic droplets as seen at 149 °C (Figure 7f). This phase transition occurs within a broad temperature range of 6 °C, as compared with a narrow range of 1 °C in the fresh sample (see Figure 5). The chain segregation and the phase separation occur also within the region in which the anisotropization has newly occurred. It gives rise to the growth of the anisotropic droplets from R_{L1} to R_{L2} and the increase of the isotropic area A_i, as seen in the image change from part f to part g of Figure 7. In this way the process involving the sequential anisotropization, chain segregation, and phase separation builds the unique spatial distribution of sizes of the anisotropic droplets as shown in parts f and g of Figure 7 which is controlled by the memory of the domain structure of parts a and b of Figure 7 which existed in the isotropic melt. The memory of the initial domain structure tends to be lost, as the coalescence of the anisotropic droplets into larger droplets and the domain reorganization progress, as is clearly indicated in parts g and h of Figure 7.

Figure 8 shows the evolution of textures in the same area as shown in Figure 7 upon further lowering of the temperature. The coalescence of the large anisotropic drops leads to wormlike anisotropic domains. These wormlike domains are more clearly seen in Figure 7h or in the micrographs obtained between 143 and 137 °C. This coalescence and the decrease of the volume fraction of the isotropic phase brought by increased anisotropization force the isotropic phase to form narrow, waving strips (or "isotropic nemas") between the anisotropic domains, as shown in parts a and b of Figure 8. At 123 °C a fully anisotropic phase is observed. This temperature is about 10 °C lower than that obtained in the fresh sample.

IV. Discussion

A. Chain Segregation and Phase Separation. For the polyester used in this study mesogens and flexible spacers are alternatively distributed along the main chain as mentioned above. All our experiments were done in a relatively low temperature interval for avoiding the chemical decomposition and the transesterification.[26] Therefore, we can believe that for the polyester the distribution of mesogens and the chemical disorder on the main chain are not the reasons for explaining the phase-separation phenomenon observed in a relatively narrow temperature interval compared with some other copolyesters.[11-13] We know that the biphase width is affected by the molecular mass of the polyester and by the molecular mass distribution.[4,7-10,16] The distribution of the molecular weight is the main reason leading to the phase separation, as shown in the previous work.[4,7-10,16]

DDA-9 used in this experiment has a polydispersity $\overline{M}_w/\overline{M}_n = 2.7$. It is the same as that for the polyester prepared by the polycondensation reaction, the parameter $\overline{M}_w/\overline{M}_n$, describing the polydispersity of polymers being likely 2–3.[34] A previous investigation done by A. Blumstein, R. B. Blumstein, and co-workers has indicated that the clearing temperature of DDA-9 is a function of the number-average molecular weight $\overline{M}_n$.[35] Therefore, it is reasonable to suppose that the polyester is a mixture formed by molecular species with the same chemical structure but different molecular lengths. For main-chain LC polymers the molecular length or the molecular contour length controls their phase transition temperature. As the molecular length is proportional to the number-average molecular weight for the main-chain LC polymers, we can obtain a correlation between the molecular weight M_n^i and the phase transition temperature $T_{N\to I}^i$ where M_n^i is the molecular weight of component i and $T_{N\to I}^i$ the corresponding phase transition temperature. If $M_n^N > ... > M_n^2 > M_n^1$, $T_{N\to I}^N > ... > T_{N\to I}^2 > T_{N\to I}^1$. If our experimental temperature T is $T_{N\to I}^N > ... T_{N\to I}^i > T > T_{N\to I}^{i-1} > T_{N\to I}^1$, a biphase region should appear in a certain temperature interval for LC polymers, like DDA-9; namely, the components with molecular weight between M_n^N and M_n^i are in the anisotropic state, but the components with molecular weight between M_n^{i-1} and M_n^1 are in the isotropic state. When an anisotropic sample is gradually heated from the fully anisotropic phase into the biphase region and the temperature is higher than T_{N-I}^i, the component i will become unstable in the nematic phase and be segregated and transported into the isotropic phase, and hence phase-separated from the anisotropic medium. The relation between x_I and the temperature obtained in the heating process of the sample, as shown in Figure 4, should reflect the molecular weight distribution of the LC polyester.

At a certain temperature T ($T > T_{N\to I}^i$) component i will lose its extended-chain conformation required to be packed in the nematic medium. The cost of the packing free energy of these chains in the nematic medium may be a possible reason for the component to be segregated out and separated from the anisotropic region. These chains form some new isotropic droplets surrounded by the nematic medium. As the chain segregation and phase separation progress, we can observe an increasing number

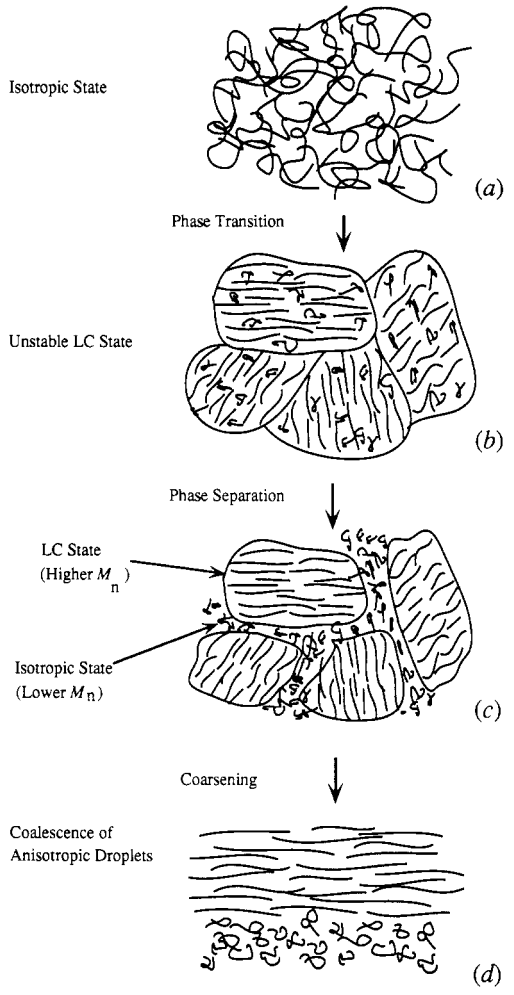

Figure 10. Schematic representation of phase transition and phase-separation processes of a fresh DDA-9 sample during the cooling process.

of isotropic droplets. The isotropic droplets grow as a consequence of a diffusion–coalescence process driven by interfacial tension between the droplets and the nematic medium. The molecules with small molecular lengths are gradually squeezed out from the anisotropic phase into the isotropic region. This occurs at different temperatures when the temperature gradually increases in heating experiments, thus leading to the molecular segregation according to molecular length in the isotropic region. Naturally we expect that a molecular weight gradient is established across the interface. The molecular weight decreases with distance from the middle of the nematic phase toward the center of the isotropic phase. This chain segregation phenomenon can be confirmed by cooling the sample again, as discussed in Figure 7. These trends are consistent with those previously obtained from DSC, NMR, and optical microscopy studies.[4,7-10,16]

B. Phase Separation Characteristic during the Cooling Process. Phase transition and phase-separation processes induced by cooling the fresh DDA-9 sample from its isotropic state are schematically represented in Figure 10. In the isotropic state, coiled chains of different lengths are randomly distributed in space on the level of the molecular size, as schematically shown in Figure 10a. After the anisotropization at a certain temperature below $T_{II \to IN}$, a texture is formed with many very small anisotropic droplets in which some molecules with a relatively long molecular length are in an extended-chain conformation, while others with a relatively short molecular length remain coiled as schematized in Figure 10b. At this stage the molecules remaining in the coiled conformation are still randomly distributed in the anisotropic medium. A seemingly full LC state can be observed by optical microscopy as shown in section III.C or as schematically illustrated in Figure 10b. The texture contains many defects around which the director orientation varies continuously, giving rise to the appearance of the very small anisotropic droplets under PLM. Though the schematic diagram in Figure 10b may give an impression of domain walls at which the orientation changes discontinuously, we do not think that this is real: the orientation is expected to change continuously according to a spatial distribution of defects. This uniform packing of the random-coiled chains in the nematic medium is energetically less stable than that of the segregated domains, as it costs packing free energy. Therefore, in order to minimize free energy, coiled molecules are separated from the anisotropic medium.

The segregated short molecules assemble in the region between anisotropic droplets, resulting in phase separation into anisotropic and isotropic domains as schematically represented in Figure 10c. The anisotropic droplets grow into larger droplets as a consequence of their diffusion–coalescence processes as shown in Figure 10d. These processes can be observed in micrographs shown in parts c–f of Figure 5. As the temperature is further lowered, the anisotropic droplets grow as a consequence of anisotropization of isotropic domains. The anisotropization occurs first in the isotropic region near the coexisting two-phase interfaces. As the anisotropization progresses, the interfaces continuously shift toward the center of the isotropic domains, as observed in Figure 7. This suggests a fractionation of molecular species in space according to their chain lengths in the biphase region; there should be a gradient in the chain-length distribution across the interface. This observation is consistent with our previous studies.[4,8] This chain length distribution in each domain should relax by remixing in the domains.[10]

Acknowledgment. W.W. gratefully acknowledges support from a scholarship for his postdoctoral research provided by the Japan Society for the Promotion of Science (ID93090). A part of this work was supported by Grants-in-Aid for Encouragement of Young Scientist-A from the Ministry of Education, Science and Culture, Japan (00093090). A.B. acknowledges the support of NSF Grant DMR-9201439.

References and Notes

(1) Blumstein, A.; Vilasagar, S. *Mol. Cryst. Liq. Cryst. (Lett.)* **1981**, *72*, 1.
(2) Blumstein, A.; Vilasagar, S.; Ponrathnam, S.; Clough, S. B.; Maret, G.; Blumstein, R. B. *J. Polym. Sci., Polym. Phys. Ed.* **1982**, *20*, 877.
(3) Blumstein, A.; Thomas, O. *Macromolecules* **1982**, *15*, 1264.
(4) Blumstein, R. B.; Blumstein, A. *Mol. Cryst. Liq. Cryst.* **1988**, *165*, 361.
(5) Antoun, S.; Lenz, R. W.; Jin, J. I. *J. Polym. Sci., Polym. Phys. Ed.* **1981**, *19*, 1901.
(6) Wunder, S. L.; Ramachadran, S.; Gochanour, C. R.; Weinberg, M. *Macromolecules* **1986**, *19*, 1696.
(7) d'Allest, J. F.; Wu, P. P.; Volino, F.; Blumstein, A.; Blumstein, R. B. *Mol. Cryst. Liq. Cryst. (Lett.)* **1986**, *3*, 103.
(8) d'Allest, J. F.; Sixou, P.; Blumstein, A.; Blumstein, R. B. *Mol. Cryst. Liq. Cryst.* **1988**, *157*, 229.
(9) Kim, D. Y.; d'Allest, J. F.; Blumstein, A.; Blumstein, R. B. *Mol. Cryst. Liq. Cryst.* **1988**, *157*, 253.
(10) Esnault, P.; Gauthier, M. M.; Volino, F.; d'Allest, J. F.; Blumstein, R. B. *Mol. Cryst. Liq. Cryst.* **1988**, *157*, 273.
(11) Martin, P. G.; Stupp, S. I. *Macromolecules* **1988**, *21*, 1222.
(12) Stupp, S. I.; Moore, J. S.; Martin, P. G. *Macromolecules* **1988**, *21*, 1228.

(13) Shiwaku, T.; Nakai, A.; Hasegawa, H.; Hashimoto, T. *Macromolecules* **1990**, *23*, 1590.
(14) Maeda, Y. *Sen-I Gakkaishi* **1991**, *47*, 392.
(15) Laus, M.; Caretti, D.; Angeloni, A. S.; Galli, G.; Chiellini, E. *Macromolecules* **1991**, *24*, 1459.
(16) Laus, M.; Angeloni, A. S.; Galli, G.; Chiellini, E. *Macromolecules* **1992**, *25*, 5301.
(17) Miller, W. G.; Wu, C. C.; Santec, G. L.; Rai, J. H.; Gaebel, K. G. *Pure Appl. Chem.* **1974**, *38*, 37.
(18) Papov, S. P.; Kulichikhin, V. G.; Kalmykova, V. D. *J. Polym. Sci., Polym. Phys. Ed.* **1974**, *12*, 1753.
(19) Panar, M.; Beste, L. F. *Polym. Prepr. (Am. Chem. Soc., Div. Polym. Chem.)* **1976**, *17* (1), 47.
(20) Matheson, R. R.; Flory, P. J. *Macromolecules* **1981**, *14*, 954.
(21) Ronca, G.; Yoon, D. Y. *J. Chem. Phys.* **1982**, *76*, 3295.
(22) ten Bosch, A.; Maissa, P. J.; Sixou, P. *J. Phys. Lett.* **1983**, *44*, 105.
(23) Khokhlov, A. R.; Semenov, A. N. *Macromolecules* **1986**, *19*, 373.
(24) Frederickson, G. H.; Leibler, L. *Macromolecules* **1990**, *23*, 531.
(25) Nakai, A.; Wang, W.; Hashimoto, T.; Blumstein, A., in preparation.
(26) Li, M. H.; Brûlet, A.; Keller, P.; Strazielle, C.; Cotton, J. P. *Macromolecules* **1993**, *26*, 119.
(27) Shiwaku, T.; Nakai, A.; Hasegawa, H.; Hashimoto, T. *Polym. Commun.* **1987**, *28*, 174.
(28) Rojstaczer, S. R.; Stein, R. S. *Macromolecules* **1990**, *23*, 4863.
(29) Wang, W.; Lieser, G.; Wegner, G. *Liq. Cryst.* **1993**, *15*, 1.
(30) Binder, K.; Stauffer, D. *Phys. Rev. Lett.* **1974**, *33*, 1006.
(31) Furukawa, H. *Progr. Theor. Phys.* **1978**, *59*, 1072; *Phys. Rev. Lett.* **1979**, *43*, 136.
(32) Hasegawa, H.; Shiwaku, T.; Nakai, A.; Hashimoto, T. In *Dynamics of Ordering Processes in Condensed Matter*; Komura, S., Furukawa, H., Eds.; Plenum: New York, 1988.
(33) Tomotika, S. *Proc. R. Soc. London, Ser. A* **1935**, *150*, 322; **1936**, *153*, 302.
(34) Flory, P. J. *Principles of Polymer Chemistry*; Cornell University Press: Ithaca, NY, 1967.
(35) Blumstein, R. B.; Stickles, E. M.; Gauthier, M. M.; Blumstein, A.; Volino, F. *Macromolecules* **1984**, *17*, 177.